R-LLaVA: Improving Med-VQA Understanding through Visual Region of Interest

Xupeng Chen[1], **Zhixin Lai**[2], **Kangrui Ruan**[3], **Shichu Chen**[1], **Jiaxiang Liu**[4*], **Zuozhu Liu**[4*]
[1]New York University, [2]Cornell University, [3]Columbia University, [4]Zhejiang University
{xc1490, sc10740}@nyu.edu
laizhixin16@gmail.com, kangruir0910app@gmail.com
{jiaxiang.21, zuozhuliu}@intl.zju.edu.cn

Abstract

Artificial intelligence has made significant strides in medical visual question answering (Med-VQA), yet prevalent studies often interpret images holistically, overlooking the visual regions of interest that may contain crucial information, potentially aligning with a doctor's prior knowledge that can be incorporated with minimal annotations (e.g., bounding boxes). To address this gap, this paper introduces R-LLaVA, designed to enhance biomedical VQA understanding by integrating simple medical annotations as prior knowledge directly into the image space through CLIP. These annotated visual regions of interest are then fed into the LLaVA model during training, aiming to enrich the model's understanding of biomedical queries. Experimental evaluation on four standard Med-VQA datasets demonstrates R-LLaVA's superiority over existing state-of-the-art (SoTA) methods. Additionally, to verify the model's capability in visual comprehension, a novel multiple-choice medical visual understanding dataset is introduced, confirming the positive impact of focusing on visual regions of interest in advancing biomedical VQA understanding.

1 Introduction

Medical Visual Question Answering (Med-VQA) has recently garnered significant attention Chen et al. (2022b); Gong et al. (2021); Ren & Zhou (2020); Khare et al. (2021). As an emerging area in medical AI, Med-VQA aims to answer medical questions in natural language based on input medical images. A robust Med-VQA system can assist clinicians in interpreting medical images, thereby ensuring accuracy and expediting the diagnostic process. For patients, automated Med-VQA services can greatly meet the demand for personalized healthcare consultations Liu et al. (2023a).

Numerous deep learning-based approaches have been explored in the realm of Med-VQA Tiong et al. (2022); Banerjee et al. (2021); Changpinyo et al. (2022); Liu et al. (2023b); Gai et al. (2024); Liu et al. (2024c). For instance, Nguyen et al. (2019) utilized Bilinear Attention Networks (BAN) Kim et al. (2018), enhancing them with Mixed Enhanced Visual Features (MEVF), which integrates pre-trained meta-learning modules and Convolutional Denoising Autoencoders (CDAE) to improve the performance of Med-VQA models. Building on this, Zhan et al. (2020) proposed a conditional reasoning framework to further enhance the inference capabilities of Med-VQA models. However, many of these methods tend to perform poorly in practical scenarios, mainly due to limitations in the extraction and integration of information from a limited number of medical images and text data Eslami et al. (2021); Song et al. (2022); Wang et al. (2022); Liu et al. (2024b; 2025). To address this, Eslami et al. (2021) introduced the CLIP architecture into the MEVF framework Nguyen et al. (2019), using CLIP as the visual encoder pre-trained in the ROCO multimodal medical dataset Pelka et al. (2018), which demonstrated significant performance gains. Additionally, Liu et al. (2023a) developed VQA-Adapter, a lightweight adapter that, combined with label smoothing, efficiently fine-tunes CLIP for Med-VQA, reducing computational costs and mitigating overfitting. Li et al. (2024) proposed LLaVA-Med, leveraging GPT-4 and a novel curriculum learning approach to efficiently train LLaVA in biomedical images, further enhancing the capabilities of Med-VQA.

* Corresponding author.

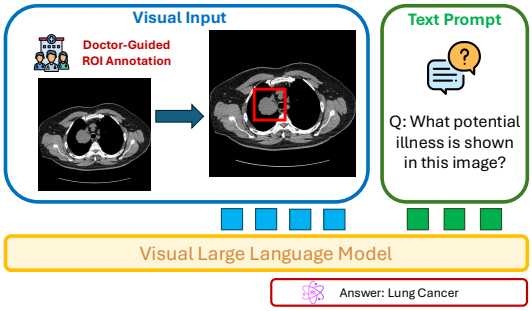

Figure 1: Integration of doctor-guided Region-of-Interest (RoI) and original image for multimodal conversational assistance. Specifically, a Doctor-Guided ROI, which is highlighted in the red box, is overlaid onto the original image in line with the clinician's diagnostic approach.

However, previous Med-VQA approaches have often overlooked the importance of medical and spatial priors that are essential for disease localization in Med-VQA tasks. Inspired by clinical practices in which doctors rely on such priors, we propose the R-LLaVA framework, which incorporates doctors' domain knowledge and spatial annotations into Med-VQA models. Fig. 1 shows the main idea of the proposed method. Specifically, we integrate simple physician annotations, such as bounding boxes (bbox), as prior knowledge, directly injecting these visual cues into the image space via CLIP showing CLIP's ability to interpret visual markers. These annotated regions are then fed into the LLaVA model during training. Our experiments show that even minimal annotations from doctors can significantly improve the accuracy of the model. R-LLaVA consistently outperforms the state-of-the-art Med-VQA methods in four large-scale datasets, demonstrating remarkable performance improvements. Our work has two major contributions:

- The work introduces R-LLaVA method to improve Med-VQA by incorporating regions of visual interest through a two-phase training process.
- To validate the model's visual comprehension, We introduce a multiple-choice medical visual understanding dataset, confirming the positive impact of integrating Visual Regions of Interest on enhancing Biomedical VQA Understanding.

2 METHOD

R-LLaVA is based on the premise that visual LLMs should analyze not only the visual content of the images themselves but also the specific regions of interest highlighted by clinicians. In this section, we detail our approach, starting with the reconstruction of medical VQA datasets to incorporate region-based information, simulating how clinicians annotate critical regions of interest. Following this strategy of dataset reconstruction, we explain the process utilized to train R-LLaVA based on these annotations.

2.1 MEDICAL DATASET RECONSTRUCTION WITH REGION-OF-INTEREST (ROI) VQA

In Med-VQA, utilizing datasets incorporating region-based information is helpful for enabling models to accurately focus on and interpret specific regions of medical images. This targeted focus ensures that model responses are grounded in the precise anatomical or pathological features of interest, leading to more accurate and clinically meaningful answers in complex medical scenarios. To evaluate and enhance the region-learning capabilities of Vision-and-Large-Language Models(VLLMs) in medical VQA tasks, we propose a strategy to reconstruct the existing medical VQA datasets by integrating RoI VQA pairs. These pairs are designed to improve and evaluate the model's ability to localize and describe specific regions within medical images.

As is shown in Fig. 2, the reconstructed dataset comprises four types of QA pairs: (1) Region localization, where the model is required to predict the bounding box coordinates corresponding to a described region, e.g., "Please provide the bounding box coordinate of the region this sentence describes: Heart". (2) Region selection - where the model is required to select the bounding box

Image	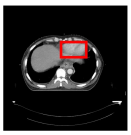	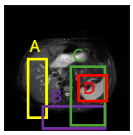		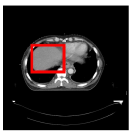
Question	Please provide the bounding box coordinate of the region this sentence describes: Heart	Select the bbox describes spleen. A. Yellow B. Purple C. Green D. Red	Please provide a short description for this region: [115, 163, 243, 268]	Please provide a short description inside the bounding box
Answer	[115, 163, 243, 268]	D. Red	Heart	Liver

Figure 2: Region-of-Interest (RoI) QA from Reconstructed VQA Dataset

among four corresponding to a described region, e.g., "Select the bounding box (bbox) describes spleen. A. Yellow B. Purple C. Green D. Red". (3) Region description with bounding box coordinates - where the model is asked to provide a description given a bounding box, e.g., "Please provide a short description for this region: [115, 163, 243, 268]". (4) Region description with Bounding Box highlighted in input image, where the model is asked to describe the bounding box, e.g., "Please provide a short description inside the bounding box".

This reconstruction of Med-VQA datasets with RoI annotations aims to push the boundaries of current VLLMs, providing a more rigorous evaluation framework for their region-learning capabilities in medical imaging tasks.

2.2 R-LLaVA Training Stage I: Pre-training

The first stage of training is to align the biomedical concepts while maintaining efficiency. As shown in Fig. 3(a), the image encoder (e.g., CLIP (Radford et al., 2021)) and the language model (e.g. Vicuna (Zheng et al., 2023)) are frozen in stage I. Only the multi-modal connector is trained by updating the projection matrix. This freezing technique is crucial for efficiency and understanding concepts, as it allows the model to connect the foundational representations of visual and textual embeddings under medical settings. The major dataset used at this stage follows the LLaVA-Med alignment dataset Li et al. (2023). It is built upon a large-scale dataset of 15 million parallel figure-caption pairs for biomedical vision-language processing—PMC-15M. PMC-15M is shrunk to only 600,000 pairs to balance concept coverage and efficiency, which speeds up training while still providing great alignment performance.

2.3 R-LLaVA Training Stage II: Instruction Tuning with Visual RoI Approach

In Stage II, the model is aimed to learn to follow various types of textual instructions across a wide range of specific medical fields and complete field-specific tasks. The model is also designed to focus on the Region-of-Interest (RoI) (e.g., bounding boxes) to enhance its vision ability for Med-VQA.

As illustrated in Fig. 3(b), during stage II, the visual encoder is frozen while the pre-trained weights of the projection layer and the language model are updated. To enhance the model's capacity for instruction-following and task execution in a biomedical conversational context, we further fine-tune the model on biomedical language-image instruction-following data, improving its ability to handle task transfer across established Med-VQA datasets.

For certain biomedical applications, it is essential to create highly accurate, dataset-specific models to meet the required performance standards. After completing the pretraining based on LLaVA-Med, we trained on four distinct Med-VQA datasets, each covering a range of dataset sizes and specialized medical topics. Given a biomedical image as input, the model is tasked with answering multiple natural language questions, generating responses in free-form text for both close-set and open-set question types.

To strengthen the model's ability to interpret arbitrary visual regions of interest, we utilize CLIP's built-in capacity to encode both the image and supplementary human-annotated visual markers. This provides enhanced guidance by merging potential doctor annotations into the image via alpha

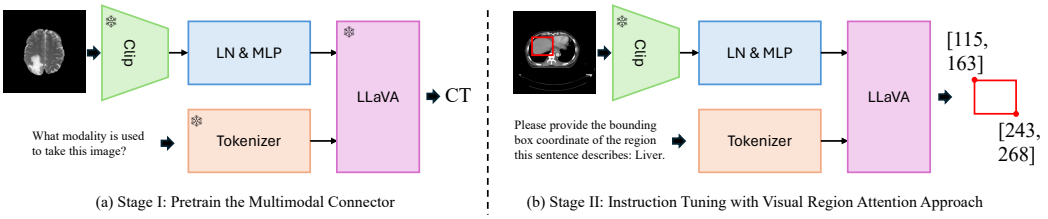

Figure 3: R-LLaVA Training Pipeline (Stage I and Stage II)

blending, drawing focus to regions of interest:

$$\bar{\mathbf{X}}_{\text{merged}} = \alpha \cdot \mathbf{P}_{\text{doc}} + (1 - \alpha) \cdot \mathbf{X}_{\text{img}}$$

where α controls the transparency level, $\mathbf{X}_{\text{img}}$ is the base image, and $\mathbf{P}_{\text{doc}}$ represents the medical regions of interest. The composite image $\bar{\mathbf{X}}_{\text{merged}}$ is then fed into the multimodal language model to guide its attention toward these key areas Vaswani et al. (2017); Dosovitskiy et al. (2021); Ruan & Di (2024).

To capture both detailed and abstract information, we extract multi-level features from several layers of CLIP. The shallower layer is used for capturing finer details, while deeper layers capture more abstract semantic representations (Ruan et al., 2024a). These features are combined, normalized using Layer Normalization for stability, and then processed by a Multi-Layer Perceptron(MLP) layer to integrate the diverse visual cues effectively.

This direct integration of visual prompts over regions of interest brings several benefits. It reduces model complexity by eliminating additional processing components and mirrors natural doctor-patient interactions, making it suitable for real-world applications.

We employ autoregressive language modeling to train the model, optimizing the likelihood of producing the ground-truth answer tokens $\mathbf{Y}$:

$$\begin{aligned} &P(\mathbf{Y} \mid \bar{\mathbf{X}}_{\text{merged}}, \mathbf{X}_{\text{instruct}}) \\ &= \prod_{t=1}^{T} P_{\mathbf{\Omega}}(x_t \mid \bar{\mathbf{X}}_{\text{merged}}, \mathbf{X}_{\text{instruct}}, \mathbf{Y}_{<t}) \end{aligned} \tag{1}$$

where $\bar{\mathbf{X}}_{\text{merged}}$ contains the integrated images with an emphasis on regions of interest, $\mathbf{X}_{\text{instruct}}$ provides the textual instruction, which can be constructed from questions. T is the sequence length of the target answer $\mathbf{Y}$, $\mathbf{Y}_{<t}$ includes all the answer tokens preceding the current prediction token x_t, and $\mathbf{\Omega}$ represents the trainable parameters.

This training approach equips the model to generate accurate and context-aware responses by integrating visual content, instructions, and visual regions of interest directed toward specific tissues, organs, and so on. This process imitates the interactions between doctors and patients by highlighting diagnostically relevant areas. It is especially effective for tasks that require a nuanced understanding of both the visual elements within a specific tissue or organ and the user's intent conveyed through certain visual markers.

3 Experiment

In this section, we first provide a detailed description of the utilized dataset (Section 3.1), including the types of questions it encompasses. Next, we present the selected evaluation metrics (Section 3.2). Based on the chosen datasets and metrics, we outline the training strategies and settings employed in our experiments (Section 3.3). We present the main results in Section 3.4, along with a comprehensive ablation study analyzing the impact of our methodological choices (Section 3.5).

3.1 Dataset

For pretraining, we utilize a large-scale medical image-caption dataset from Li et al. (2024), containing 600K pairs to facilitate foundational alignment with medical concepts. For Fine-tuning, we employ

four VQA datasets: VQA-RAD, SLAKE-EN, PathVQA, and VQA-Med. We augment the SLAKE-EN dataset with RoI QA, as detailed in Section 2.1. We adopt a consistent 80/20 train-test split for all datasets, including VQA-RAD, SLAKE-EN, PathVQA, and VQA-Med 2019.

We define three question types: close-ended, multi-choice, and open-ended. Close-ended questions yield straightforward answers, typically "Yes" or "No" (e.g., "Is there any abnormality in the spleen?"). Multi-choice questions provide a set of predefined answers (e.g., "Which rectangle contains the object representing Cardiomegaly?"). Open-ended questions solicit descriptive responses (e.g. "Please provide a short description for this region").

	VQA-RAD		**SLAKE-EN**			**PathVQA**		**VQA-Med 2019**	**Act.**
Method	Open	Closed	Open	Closed	Multi	Open	Closed	Closed	
Performance of prior methods with reported metrics in the study									
CGMVQA Ens. Ren & Zhou (2020)	-	-	-	-	-	-	-	<u>78.10</u>	-
MMBERT Khare et al. (2021)	-	77.90	-	-	-	-	-	<u>78.10</u>	-
M2I2 (Li et al., 2022a)	-	83.50	-	91.10	-	-	88.00	-	-
CLIP-ViT w/ GPT2-XL Van Sonsbeek et al. (2023)	-	-	84.30	82.10	-	40.0	87.00	-	-
VL Encoder–Decoder (Bazi et al., 2023b)	-	82.47	-	-	-	-	85.61	-	-
Q2ATransformer (Liu et al., 2023c)	-	81.20	-	-	-	54.85	88.85	-	-
Prefix T. Medical LM (Van Sonsbeek et al., 2023)	-	-	-	82.01	-	-	87.00	-	-
PubMedCLIP (Eslami et al., 2023b)	-	80.00	-	82.50	-	-	-	-	-
BiomedCLIP (Zhang et al., 2023b)	-	79.80	-	89.70	-	-	-	-	-
BiomedGPT-S (Zhang et al., 2023a)	13.40	57.80	66.50	73.30	-	10.70	84.20	-	-
BiomedGPT-M (Zhang et al., 2023a)	53.60	65.07	78.30	86.80	-	12.5	85.70	-	-
Gemini Pro Yang et al. (2024)	-	60.29	-	72.60	-	-	60.22	70.30	-
Supervised finetuning results									
LLaVA Liu et al. (2024a)	50.00	65.07	78.18	63.22	-	7.74	63.20	-	7B
LLaVA-Med (LLama7B) Li et al. (2024)	61.52	**84.19**	83.08	<u>85.34</u>	-	37.95	91.21	-	7B
LLaVA-Med (Vicuna7B) Li et al. (2024)	<u>64.39</u>	81.98	<u>84.71</u>	83.17	<u>40.85</u>	**38.87**	<u>91.65</u>	-	7B
LLaVA-Med (Phi2.7B) Li et al. (2024)	54.83	81.35	81.29	83.29	-	31.73	90.17	-	2.7B
R-LLaVA (7B)	**64.91**	<u>83.76</u>	**89.47**	**90.13**	**68.85**	<u>38.24</u>	**92.59**	**80.97**	7B

Table 1: Performance on Med-VQA tasks. **Bold** denotes the best performance; <u>underlined</u> denotes the second-best.

3.2 METRICS

For close-ended and multi-choice questions, we use accuracy as the evaluation metric, assessing it by directly comparing predictions with ground truth. For open-ended questions, we measure recall, calculating the proportion of ground-truth tokens present in the generated sequences (Chen et al., 2024; Jiang et al., 2024).

3.3 TRAINING STRATEGY AND SETTING

We use CLIP-ViT-L/14@336px Radford et al. (2021) as the vision encoder to extract relevant features from input medical images, and Vicuna 1.5 Chiang et al. (2023) as the language model. A 2-layer MLP serves as the multi-modal projector.

Stage I: Pretraining. The 2-layer multimodal projector is pre-trained on large-scale medical image-caption pairs, developing a foundational understanding of visual data without instruction-following abilities. The training uses a batch size of 256, a learning rate of 1×10^{-3}, and a maximum sequence length of 2048 tokens for 1 epoch without weight decay.

Stage II: Instruction Fine-Tuning. With the CLIP encoder fixed, we fine-tune the remaining model components on specialized biomedical instruction-following data (up to 60K samples) with diverse queries and inline mentions, enhancing performance across medical domains. This stage uses a batch size of 128, a reduced learning rate of 2×10^{-5}, and a maximum sequence length of 2048 tokens, trained for 1 epoch without weight decay.

Both pretraining and fine-tuning stages are conducted on 8 A100 80G GPUs. Pretraining requires approximately 6 hours for the 7B model and 12 hours for the 13B model, while fine-tuning takes 3 hours for the 7B model and 6 hours for the 13B model. All models use FP16 precision for both training and inference.

3.4 MAIN RESULTS

Quantitative Comparison The experimental results in Table 1 demonstrate that our proposed model, R-LLaVA(7B), sets a new state-of-the-art on several medical visual question answering (VQA)

benchmarks. Specifically, R-LLaVA(7B) achieves the best performance on SLAKE-EN, with an accuracy of 89.47% on open-ended questions and 90.13% on close-ended questions, outperforming all competing models by a significant margin. This highlights the effectiveness of our region of interest approach. Furthermore, R-LLaVA(7B) also delivers superior results on VQA-Med 2019, achieving an accuracy of 80.97% on close-ended questions. For the VQA-RAD and PathVQA datasets, our model consistently achieves superiority on both open-ended and closed-ended tasks, reinforcing its robustness across diverse medical VQA challenges.

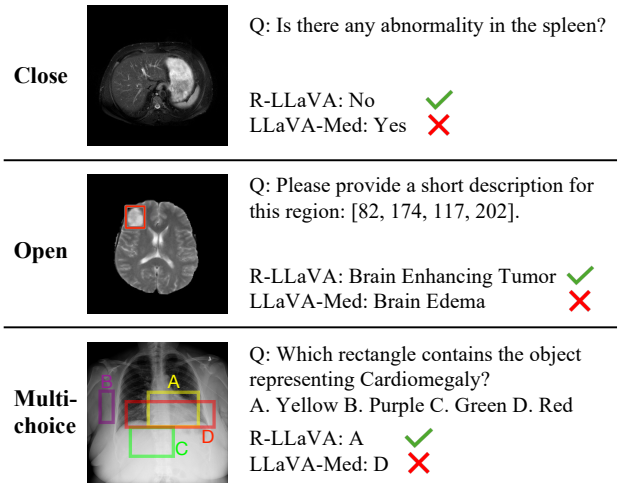

Figure 4: Qualitative comparison of medical visual question answering on three types of questions from SLAKE dataset.

			VQA-RAD		SLAKE-EN			PathVQA		Med 2019
Data	Init	Size	Open	Closed	Open	Closed	Multi	Open	Closed	Closed
single	ViP-LLaVA	7B	62.78	80.27	88.61	88.94	**70.65**	35.63	91.02	80.35
single	ViP-LLaVA	13B	60.58	77.19	87.07	85.54	66.57	36.4	90.35	77.51
single	Vicuna	7B	62.26	78.17	87.55	88.55	68.34	32.97	90.93	79.38
single	Vicuna	13B	58.3	76.13	85.99	86.58	64.47	33.92	89.17	76.2
all	ViP-LLaVA	7B	**64.91**	83.76	**89.47**	**90.13**	68.85	**38.24**	**92.59**	**80.97**
all	ViP-LLaVA	13B	63.49	**84.31**	87.14	87.31	69.14	36.29	90.7	79.14
all	Vicuna	7B	59.99	80.64	87.28	89.48	67.25	37.21	91.51	77.69
all	Vicuna	13B	57.15	81.03	86.31	88.44	65.33	35.22	89.32	77.79

Table 2: Ablation Studies on Model Choices

		VQA-RAD		SLAKE-EN			PathVQA		Med 2019
Pretrain	Finetune	Open	Closed	Open	Closed	Multi	Open	Closed	Closed
✗	✗	20.74	59.19	26.82	50.24	-	8.74	45.65	-
✓	✗	27.88	57.81	40.05	45.22	27.49	14.25	50.53	42.38
✗	✓	50.25	64.53	70.27	73.97	50.73	22.84	60.49	58.67
✓	✓	**64.91**	**83.76**	**89.47**	**90.13**	**68.85**	**38.24**	**92.59**	**80.97**

Table 3: Ablation Studies on Training Strategies

Qualitative Comparison From Fig. 4, R-LLaVA demonstrates superior performance over LLaVA-Med across all question types. Specifically, for close-ended questions, such as identifying abnormalities in specific organs (e.g., spleen), R-LLaVA provides more accurate responses. For open-ended questions that require descriptive answers, R-LLaVA accurately describes specific regions with detailed terms closely aligned to medical findings. For example, it correctly identifies a "Brain Enhancing Tumor," demonstrating a deeper understanding of the medical context, whereas LLaVA-Med misclassifies it as "Brain Edema," highlighting a gap in spatial and contextual comprehension. In multi-choice scenarios, R-LLaVA consistently selects the correct bounding box corresponding to medical conditions like cardiomegaly. Its precision in choosing the right option reflects its effective

use of attention-based mechanisms to interpret complex image regions, surpassing LLaVA-Med's less consistent performance. These quantitative and qualitative results underscore R-LLaVA's enhanced ability to handle the nuanced demands of Med-VQA tasks.

3.5 ABLATION STUDY

In this section, we evaluate the effectiveness of each component in the model training process, covering model selection, two-stage training strategy, and the visual Region-of-Interest (RoI) approach.

3.5.1 MODEL SELECTION

We first conducted an ablation study on model configurations, focusing on whether the initial parameters were loaded from **Vicuna** (Zheng et al., 2023) or **ViP-LLaVA** (Cai et al., 2024). Additionally, we compared two fine-tuning strategies: *single* and *all*. In the *single* strategy, the model is trained and evaluated independently on each dataset. In contrast, the *all* strategy involves training the model on all datasets collectively, enabling it to generalize and better understand medical prompts across different datasets. Furthermore, we evaluated two model sizes: **7B** and **13B**.

As shown in Table 2, the 7B model, initialized with parameters from ViP-LLaVA and fine-tuned on data from all four datasets, achieves the best performance.

		VQA-RAD		**SLAKE-EN**			**PathVQA**		**Med 2019**
Bbox in Prompt	alpha	Open	Closed	Open	Closed	Multi	Open	Closed	Closed
✗	$\alpha = 0$	63.26	82.22	80.39	81.32	31.06	34.47	90.69	77.13
✓	$\alpha = 0$	63.05	82.11	83.41	81.86	25.22	35.78	89.68	78.91
✓	$\alpha = 96$	64.73	83.09	88.65	89.32	65.32	36.84	90.95	80.12
✓	$\alpha = 128$	64.49	82.57	88.88	88.98	67.41	37.11	90.47	80.31
✓	$\alpha = 255$	64.79	82.72	89.69	89.08	67.83	37.50	91.84	80.79
✓	Dynamic	**64.91**	**83.76**	**89.47**	**90.13**	**68.85**	**38.24**	**92.59**	**80.97**

Table 4: Ablation Studies on Region-of-Interest (RoI) Approach

3.5.2 TWO-STAGE TRAINING STRATEGY

We demonstrate the importance of both training stages: pretraining on the LLaVA-Med dataset and fine-tuning across four VQA datasets.

From Table 3, we observe that without pretraining and fine-tuning (row 1), the model achieves very low accuracy across all four datasets, with open-ended question accuracy below 30% on the first three datasets and only 8.74% on PathVQA. With pretraining only (row 2) or fine-tuning only (row 3), the performance improves. Fine-tuning alone generally yields better results across all datasets compared to pretraining alone; for instance, it achieves an accuracy of 70.27% on SLAKE-EN open-ended questions versus 40.05% for pretraining only and 26.82% without any training. However, pretraining only slightly reduces accuracy on close-ended questions (57.81% for VQA-RAD and 45.22% for SLAKE-EN) compared to the baseline without training (59.19% for VQA-RAD and 50.24% for SLAKE-EN). With both training stages (row 4), our model achieves optimal results, showing double-digit improvements across various question types and datasets compared to other experiments.

Our findings highlight the importance of performing both pretraining and fine-tuning. Fine-tuning enables the model to acquire task-specific abilities, while pretraining provides essential background knowledge on domain-specific topics, which significantly enhances the performance compared to fine-tuning alone.

3.5.3 VISUAL REGION-OF-INTEREST (ROI) APPROACH

We demonstrate the effectiveness of the visual RoI approach through both quantitative results in Table 4 and qualitative results in Fig. 4. In Table 4, "Bbox in Prompt" means adding bounding box information in the prompt, and "alpha" is the weight of alpha blending.

Visual Region-of-Interest (RoI) Approach From Table 4, without bounding box information in both prompt and input image (Row 1), we observe an accuracy of 80.39% on open-ended questions, 81.32% on close-ended questions, and 31.06% on multi-choice questions for the SLAKE-EN dataset. The lack of bounding box information in both the prompt and input image results in lower performance across all datasets, particularly in the multi-choice questions, than in the experiments with Visual RoI (Row 3, 4, 5, 6). Adding bounding box information in the prompt while keeping alpha at 0 based on Row 1, Row 2 slightly improves performance across open-ended questions (83.41%) and close-ended questions (81.86%) in SLAKE-EN, with a minor boost in multi-choice questions (25.22%). This indicates that bounding box prompts contribute positively but are insufficient alone.

These findings demonstrate that the visual RoI approach, which incorporates bounding boxes in both the prompt and input image, is critical for enhancing model performance on VQA datasets, particularly in the multi-choice categories of SLAKE-EN.

Alpha Blending Strategy This experiment analyzes the impact of varying bounding box opacity (alpha) on VQA performance across multiple datasets. Higher alpha values represent a more visible bounding box, while lower values signify a subtler presence. Alpha values include fixed levels (96, 128, 255) and a randomly sampled range within [96, 255]. For all VQA datasets, alpha values of 96, 128, and 255 yield similar results, with slight incremental improvements as alpha increases. This suggests that a more visible bounding box can aid in certain tasks but may not significantly influence outcomes. Randomized Alpha (Dynamic) within the range [96, 255] achieves the best results across all VQA datasets compared to other fixed alpha groups. The variability introduced by random alpha values likely provides a more robust learning experience by exposing the model to diverse bounding box appearances, resulting in improved generalization and accuracy.

4 Related Work

4.1 Visual Large Language Model

Recent years have witnessed significant advancements in Large Language Models (LLMs) Brown et al. (2020). Concurrently, developments in Large Vision Models (LVMs) have emerged, complementing LLMs through their capacity for visual understanding. Integrating multimodal understanding into large language models has significantly advanced multimodal AI capabilities Ruan et al. (2024b; 2025). Early models like ViLBERT Lu et al. (2019) and VisualBERT Li et al. (2019) extended the BERT architecture to process both text and images, enabling tasks such as visual question answering and image captioning. Contrastive learning frameworks like CLIP Radford et al. (2021) learned joint representations of images and text from large-scale datasets, achieving impressive zero-shot performance on various tasks. Recent developments focus on a more seamless integration of vision and language. Models like Flamingo Alayrac et al. (2022) and PaLI Chen et al. (2022a) incorporate visual information into language models using gated cross-attention and scale-up pre-training with multilingual data. Furthermore, the enhanced multimodal features of ChatGPT and Gemini Team et al. (2023) model represent significant strides toward more integrated and capable AI systems.

4.2 Med-VQA

Med-VQA is a method where a model answers questions from patients or clinicians based on medical images like CT scans, MRI scans, or pathology images. With the advancement of deep learning, researchers have proposed numerous Med-VQA methods. M2I2 Li et al. (2022b) is a self-supervised vision-language pretraining method that significantly improves medical VQA performance by learning multimodal representations through masked modeling and contrastive learning. However, its ability to predict free-form answers may be influenced by the complexity of the dataset. BiomedCLIP Zhang et al. (2024) is a multimodal biomedical foundation model trained on PMC-15M. It outperforms earlier vision-language models like PubMedCLIP Eslami et al. (2023a) and MedCLIP, as well as radiology-specific models such as BioViL Boecking et al. (2022). Bazi Bazi et al. (2023a) proposes a vision-language model based on a Transformer encoder-decoder architecture. It leverages the CLIP model for semantic embedding and uses a generative decoder to produce answers in an autoregressive manner. Recently, inspired by LLaVA (Liu et al., 2024a), LLaVA-Med (Li et al., 2024) fine-tunes LLaVA by self-generated biomedical instruction-following dataset to address challenges in medical

image interpretation. However, the explicit handling of region-specific information in complex medical scenarios remains insufficiently explored.

5 CONCLUSION

In this paper, we introduce R-LLaVA, an effective method to enhance Med-VQA understanding by leveraging Visual Regions of Interest. This approach integrates simple physician annotations, such as bounding boxes, as prior knowledge, directly infusing these visual cues into the image space via CLIP. During training, these annotated Visual Regions of Interest are fed into the LLaVA model to boost Biomedical VQA Understanding. A specially constructed multiple-choice dataset demonstrates the positive impact of Visual Regions of Interest within R-LLaVA. Experimental results on four Med-VQA datasets show that R-LLaVA outperforms existing SoTA techniques, significantly surpassing recent methods.

LIMITATION

Based on our experiments, we demonstrate that even minimal annotations provided by doctors can significantly enhance the accuracy of R-LLaVA. While doctor-specified regions of interest are not required during inference—R-LLaVA is capable of processing both annotated and non-annotated cases—some degree of annotation is necessary during the training phase to achieve optimal performance. Additionally, we conducted a series of ablation studies examining model configurations, training strategies, and the inclusion of visual regions of interest. These studies consistently showed that the proposed method outperforms baseline approaches, particularly in clinical scenarios where visual region annotations are utilized.

POTENTIAL RISKS AND BROADER IMPACTS

The proposed method, which builds on LLaVA (Liu et al., 2024a; Cai et al., 2024), inherits several inherent challenges associated with VLLMs, such as hallucination and biases. Regarding hallucination, as demonstrated in Table 1 and Fig. 4, R-LLaVA makes more effective use of the visual regions of interest, leading to generally superior performance. Nevertheless, it may still produce responses that are not grounded in factual information or the input data. We consider this work a significant step toward enhancing biomedical VQA by utilizing doctor guidance. To address potential biases (Ruan et al., 2023), particularly those that could favor or disfavor specific demographics, we test R-LLaVA on cases where annotations were unavailable due to privacy constraints. Additionally, integrating improved vision or language encoders could further alleviate these biases. Given the high computational cost and energy demand of training LLMs in general, we leverage pre-trained image and language encoders. This approach is especially appropriate given the relatively small size of biomedical datasets, eliminating the need for training from scratch.

In particular, R-LLaVA could democratize access to expert-level biomedical information, offering non-specialists—such as primary care physicians, medical trainees, and even patients themselves—an enhanced tool for understanding complex medical data. This capability is crucial in low-resource settings where access to specialized medical expertise is limited, thus reducing healthcare disparities on a global scale. Furthermore, by enabling more accurate and contextually grounded responses, the model could assist clinicians in making more informed, evidence-based decisions, potentially improving patient outcomes and reducing diagnostic errors.

In summary, the proposed method not only advances the technical status of biomedical VQA but also holds promise for generating significant social benefits, particularly by improving healthcare accessibility, reducing disparities, and promoting AI development. These contributions align with the growing emphasis on the ethical and socially responsible deployment of AI in sensitive domains such as healthcare.

REFERENCES

Jean-Baptiste Alayrac, Jeff Donahue, Pauline Luc, Antoine Miech, Iain Barr, Yana Hasson, Karel Lenc, Arthur Mensch, Katherine Millican, Malcolm Reynolds, et al. Flamingo: a visual language model for few-shot learning. *Advances in neural information processing systems*, 35:23716–23736, 2022.

Pratyay Banerjee, Tejas Gokhale, Yezhou Yang, and Chitta Baral. Weaqa: Weak supervision via captions for visual question answering. *Findings of the Association for Computational Linguistics: ACL-IJCNLP 2021*, 2021.

Yakoub Bazi, Mohamad Al Rahhal, Laila Bashmal, and Mansour Zuair. Vision–language model for visual question answering in medical imagery. *Bioengineering*, 10, 03 2023a. doi: 10.3390/bioengineering10030380.

Yakoub Bazi, Mohamad Mahmoud Al Rahhal, Laila Bashmal, and Mansour Zuair. Vision–language model for visual question answering in medical imagery. *Bioengineering*, 10(3):380, 2023b.

Benedikt Boecking, Naoto Usuyama, Shruthi Bannur, Daniel C. Castro, Anton Schwaighofer, Stephanie Hyland, Maria Wetscherek, Tristan Naumann, Aditya Nori, Javier Alvarez-Valle, Hoifung Poon, and Ozan Oktay. *Making the Most of Text Semantics to Improve Biomedical Vision–Language Processing*, pp. 1–21. Springer Nature Switzerland, 2022. ISBN 9783031200595. doi: 10.1007/978-3-031-20059-5_1. URL http://dx.doi.org/10.1007/978-3-031-20059-5_1.

Tom Brown, Benjamin Mann, Nick Ryder, Melanie Subbiah, Jared D Kaplan, Prafulla Dhariwal, Arvind Neelakantan, Pranav Shyam, Girish Sastry, Amanda Askell, et al. Language models are few-shot learners. *Advances in neural information processing systems*, 33:1877–1901, 2020.

Mu Cai, Haotian Liu, Siva Karthik Mustikovela, Gregory P Meyer, Yuning Chai, Dennis Park, and Yong Jae Lee. Vip-llava: Making large multimodal models understand arbitrary visual prompts. In *Proceedings of the IEEE/CVF Conference on Computer Vision and Pattern Recognition*, pp. 12914–12923, 2024.

Soravit Changpinyo, Doron Kukliansy, Idan Szpektor, Xi Chen, Nan Ding, and Radu Soricut. All you may need for vqa are image captions. In *Proceedings of the 2022 Conference of the North American Chapter of the Association for Computational Linguistics: Human Language Technologies*, pp. 1947–1963, 2022.

Shaoxiang Chen, Zequn Jie, and Lin Ma. Llava-mole: Sparse mixture of lora experts for mitigating data conflicts in instruction finetuning mllms. *arXiv preprint arXiv:2401.16160*, 2024.

Xi Chen, Xiao Wang, Soravit Changpinyo, AJ Piergiovanni, Piotr Padlewski, Daniel Salz, Sebastian Goodman, Adam Grycner, Basil Mustafa, Lucas Beyer, et al. Pali: A jointly-scaled multilingual language-image model. *arXiv preprint arXiv:2209.06794*, 2022a.

Zhihong Chen, Guanbin Li, and Xiang Wan. Align, reason and learn: Enhancing medical vision-and-language pre-training with knowledge. In *Proceedings of the 30th ACM International Conference on Multimedia*, pp. 5152–5161, 2022b.

Wei-Lin Chiang, Zhuohan Li, Zi Lin, Ying Sheng, Zhanghao Wu, Hao Zhang, Lianmin Zheng, Siyuan Zhuang, Yonghao Zhuang, Joseph E Gonzalez, et al. Vicuna: An open-source chatbot impressing gpt-4 with 90%* chatgpt quality. *See https://vicuna. lmsys. org (accessed 14 April 2023)*, 2(3):6, 2023.

Alexey Dosovitskiy, Lucas Beyer, Alexander Kolesnikov, Dirk Weissenborn, Xiaohua Zhai, Thomas Unterthiner, Mostafa Dehghani, Matthias Minderer, Georg Heigold, Sylvain Gelly, Jakob Uszkoreit, and Neil Houlsby. An image is worth 16x16 words: Transformers for image recognition at scale. *ICLR*, 2021.

Sedigheh Eslami, Gerard de Melo, and Christoph Meinel. Does clip benefit visual question answering in the medical domain as much as it does in the general domain? *arXiv preprint arXiv:2112.13906*, 2021.

Sedigheh Eslami, Christoph Meinel, and Gerard de Melo. PubMedCLIP: How much does CLIP benefit visual question answering in the medical domain? In Andreas Vlachos and Isabelle Augenstein (eds.), *Findings of the Association for Computational Linguistics: EACL 2023*, pp. 1181–1193, Dubrovnik, Croatia, May 2023a. Association for Computational Linguistics. doi: 10.18653/v1/2023.findings-eacl.88. URL https://aclanthology.org/2023.findings-eacl.88.

Sedigheh Eslami, Christoph Meinel, and Gerard De Melo. Pubmedclip: How much does clip benefit visual question answering in the medical domain? In *Findings of the Association for Computational Linguistics: EACL 2023*, pp. 1151–1163, 2023b.

Xiaotang Gai, Chenyi Zhou, Jiaxiang Liu, Yang Feng, Jian Wu, and Zuozhu Liu. Medthink: Explaining medical visual question answering via multimodal decision-making rationale. *arXiv preprint arXiv:2404.12372*, 2024.

Haifan Gong, Guanqi Chen, Sishuo Liu, Yizhou Yu, and Guanbin Li. Cross-modal self-attention with multi-task pre-training for medical visual question answering. In *Proceedings of the 2021 International Conference on Multimedia Retrieval*, pp. 456–460, 2021.

Albert Q Jiang, Alexandre Sablayrolles, Antoine Roux, Arthur Mensch, Blanche Savary, Chris Bamford, Devendra Singh Chaplot, Diego de las Casas, Emma Bou Hanna, Florian Bressand, et al. Mixtral of experts. *arXiv preprint arXiv:2401.04088*, 2024.

Yash Khare, Viraj Bagal, Minesh Mathew, Adithi Devi, U Deva Priyakumar, and CV Jawahar. Mmbert: Multimodal bert pretraining for improved medical vqa. In *2021 IEEE 18th International Symposium on Biomedical Imaging (ISBI)*, pp. 1033–1036. IEEE, 2021.

Jin-Hwa Kim, Jaehyun Jun, and Byoung-Tak Zhang. Bilinear attention networks. *Advances in neural information processing systems*, 31, 2018.

Chunyuan Li, Cliff Wong, Sheng Zhang, Naoto Usuyama, Haotian Liu, Jianwei Yang, Tristan Naumann, Hoifung Poon, and Jianfeng Gao. Llava-med: Training a large language-and-vision assistant for biomedicine in one day, 2023. URL https://arxiv.org/abs/2306.00890.

Chunyuan Li, Cliff Wong, Sheng Zhang, Naoto Usuyama, Haotian Liu, Jianwei Yang, Tristan Naumann, Hoifung Poon, and Jianfeng Gao. Llava-med: Training a large language-and-vision assistant for biomedicine in one day. *Advances in Neural Information Processing Systems*, 36, 2024.

Liunian Harold Li, Mark Yatskar, Da Yin, Cho-Jui Hsieh, and Kai-Wei Chang. Visualbert: A simple and performant baseline for vision and language. *arXiv preprint arXiv:1908.03557*, 2019.

Pengfei Li, Gang Liu, Lin Tan, Jinying Liao, and Shenjun Zhong. Self-supervised vision-language pretraining for medical visual question answering. *arXiv preprint arXiv:2211.13594*, 2022a.

Pengfei Li, Gang Liu, Lin Tan, Jinying Liao, and Shenjun Zhong. Self-supervised vision-language pretraining for medical visual question answering, 2022b. URL https://arxiv.org/abs/2211.13594.

Haotian Liu, Chunyuan Li, Qingyang Wu, and Yong Jae Lee. Visual instruction tuning. *Advances in neural information processing systems*, 36, 2024a.

Jiaxiang Liu, Tianxiang Hu, Yan Zhang, Yang Feng, Jin Hao, Junhui Lv, and Zuozhu Liu. Parameter-efficient transfer learning for medical visual question answering. *IEEE Transactions on Emerging Topics in Computational Intelligence*, 2023a.

Jiaxiang Liu, Tianxiang Hu, Yan Zhang, Xiaotang Gai, YANG FENG, and Zuozhu Liu. A chatgpt aided explainable framework for zero-shot medical image diagnosis. In *ICML 3rd Workshop on Interpretable Machine Learning in Healthcare (IMLH)*, 2023b.

Jiaxiang Liu, Tianxiang Hu, Huimin Xiong, Jiawei Du, Yang Feng, Jian Wu, Joey Zhou, and Zuozhu Liu. Vpl: Visual proxy learning framework for zero-shot medical image diagnosis. In *Findings of the Association for Computational Linguistics: EMNLP 2024*, pp. 9978–9992, 2024b.

Jiaxiang Liu, Yuan Wang, Jiawei Du, Joey Tianyi Zhou, and Zuozhu Liu. MedCoT: Medical chain of thought via hierarchical expert. In Yaser Al-Onaizan, Mohit Bansal, and Yun-Nung Chen (eds.), *Proceedings of the 2024 Conference on Empirical Methods in Natural Language Processing*, pp. 17371–17389, Miami, Florida, USA, November 2024c. Association for Computational Linguistics. doi: 10.18653/v1/2024.emnlp-main.962. URL https://aclanthology.org/2024.emnlp-main.962/.

Jiaxiang Liu, Tianxiang Hu, Jiawei Du, Ruiyuan Zhang, Joey Tianyi Zhou, and Zuozhu Liu. Kpl: Training-free medical knowledge mining of vision-language models. *arXiv preprint arXiv:2501.11231*, 2025.

Yunyi Liu, Zhanyu Wang, Dong Xu, and Luping Zhou. Q2atransformer: Improving medical vqa via an answer querying decoder. *arXiv preprint arXiv:2304.01611*, 2023c.

Jiasen Lu, Dhruv Batra, Devi Parikh, and Stefan Lee. Vilbert: Pretraining task-agnostic visiolinguistic representations for vision-and-language tasks. *Advances in neural information processing systems*, 32, 2019.

Binh D Nguyen, Thanh-Toan Do, Binh X Nguyen, Tuong Do, Erman Tjiputra, and Quang D Tran. Overcoming data limitation in medical visual question answering. In *International Conference on Medical Image Computing and Computer-Assisted Intervention*, pp. 522–530. Springer, 2019.

Obioma Pelka, Sven Koitka, Johannes Rückert, Felix Nensa, and Christoph M Friedrich. Radiology objects in context (roco): a multimodal image dataset. In *Intravascular Imaging and Computer Assisted Stenting and Large-Scale Annotation of Biomedical Data and Expert Label Synthesis: 7th Joint International Workshop, CVII-STENT 2018 and Third International Workshop, LABELS 2018, Held in Conjunction with MICCAI 2018, Granada, Spain, September 16, 2018, Proceedings 3*, pp. 180–189. Springer, 2018.

Alec Radford, Jong Wook Kim, Chris Hallacy, Aditya Ramesh, Gabriel Goh, Sandhini Agarwal, Girish Sastry, Amanda Askell, Pamela Mishkin, Jack Clark, et al. Learning transferable visual models from natural language supervision. In *International conference on machine learning*, pp. 8748–8763. PMLR, 2021.

Fuji Ren and Yangyang Zhou. Cgmvqa: A new classification and generative model for medical visual question answering. *IEEE Access*, 8:50626–50636, 2020.

Kangrui Ruan and Xuan Di. Infostgcan: An information-maximizing spatial-temporal graph convolutional attention network for heterogeneous human trajectory prediction. *Computers*, 13(6):151, 2024.

Kangrui Ruan, Junzhe Zhang, Xuan Di, and Elias Bareinboim. Causal imitation learning via inverse reinforcement learning. In *The Eleventh International Conference on Learning Representations*, 2023.

Kangrui Ruan, Xin He, Jiyang Wang, Xiaozhou Zhou, Helian Feng, and Ali Kebarighotbi. S2e: Towards an end-to-end entity resolution solution from acoustic signal. In *ICASSP 2024-2024 IEEE International Conference on Acoustics, Speech and Signal Processing (ICASSP)*, pp. 10441–10445. IEEE, 2024a.

Kangrui Ruan, Xinyang Wang, and Xuan Di. From twitter to reasoner: Understand mobility travel modes and sentiment using large language models. *arXiv preprint arXiv:2411.02666*, 2024b.

Kangrui Ruan, Junzhe Zhang, Xuan Di, and Elias Bareinboim. Causal imitation for markov decision processes: A partial identification approach. *Advances in Neural Information Processing Systems*, 37:87592–87620, 2025.

Haoyu Song, Li Dong, Weinan Zhang, Ting Liu, and Furu Wei. Clip models are few-shot learners: Empirical studies on vqa and visual entailment. In *Proceedings of the 60th Annual Meeting of the Association for Computational Linguistics (Volume 1: Long Papers)*, pp. 6088–6100, 2022.

Gemini Team, Rohan Anil, Sebastian Borgeaud, Yonghui Wu, Jean-Baptiste Alayrac, Jiahui Yu, Radu Soricut, Johan Schalkwyk, Andrew M Dai, Anja Hauth, et al. Gemini: a family of highly capable multimodal models. *arXiv preprint arXiv:2312.11805*, 2023.

Anthony Meng Huat Tiong, Junnan Li, Boyang Li, Silvio Savarese, and Steven C.H. Hoi. Plug-and-play VQA: Zero-shot VQA by conjoining large pretrained models with zero training. In *Findings of the Association for Computational Linguistics: EMNLP 2022*, pp. 951–967, Abu Dhabi, United Arab Emirates, December 2022. Association for Computational Linguistics. URL https://aclanthology.org/2022.findings-emnlp.67.

Tom Van Sonsbeek, Mohammad Mahdi Derakhshani, Ivona Najdenkoska, Cees GM Snoek, and Marcel Worring. Open-ended medical visual question answering through prefix tuning of language models. In *International Conference on Medical Image Computing and Computer-Assisted Intervention*, pp. 726–736. Springer, 2023.

Ashish Vaswani, Noam Shazeer, Niki Parmar, Jakob Uszkoreit, Llion Jones, Aidan N Gomez, Łukasz Kaiser, and Illia Polosukhin. Attention is all you need. *Advances in neural information processing systems*, 30, 2017.

Zhecan Wang, Bin Xiao, Noel Codella, Jianwei Yang, Yen-Chun Chen, Luowei Zhou, Shih-Fu Chang, Xiyang Dai, Haoxuan You, and Lu Yuan. Clip-td: Clip targeted distillation for vision-language tasks. In *International Conference on Learning Representations*, 2022.

Lin Yang, Shawn Xu, Andrew Sellergren, Timo Kohlberger, Yuchen Zhou, Ira Ktena, Atilla Kiraly, Faruk Ahmed, Farhad Hormozdiari, Tiam Jaroensri, et al. Advancing multimodal medical capabilities of gemini. *arXiv preprint arXiv:2405.03162*, 2024.

Li-Ming Zhan, Bo Liu, Lu Fan, Jiaxin Chen, and Xiao-Ming Wu. Medical visual question answering via conditional reasoning. In *Proceedings of the 28th ACM International Conference on Multimedia*, pp. 2345–2354, 2020.

Kai Zhang, Jun Yu, Zhiling Yan, Yixin Liu, Eashan Adhikarla, Sunyang Fu, Xun Chen, Chen Chen, Yuyin Zhou, Xiang Li, et al. Biomedgpt: A unified and generalist biomedical generative pre-trained transformer for vision, language, and multimodal tasks. *arXiv preprint arXiv:2305.17100*, 2023a.

Sheng Zhang, Yanbo Xu, Naoto Usuyama, Jaspreet Bagga, Robert Tinn, Sam Preston, Rajesh Rao, Mu Wei, Naveen Valluri, Cliff Wong, et al. Large-scale domain-specific pretraining for biomedical vision-language processing. *arXiv preprint arXiv:2303.00915*, 2023b.

Sheng Zhang, Yanbo Xu, Naoto Usuyama, Hanwen Xu, Jaspreet Bagga, Robert Tinn, Sam Preston, Rajesh Rao, Mu Wei, Naveen Valluri, Cliff Wong, Andrea Tupini, Yu Wang, Matt Mazzola, Swadheen Shukla, Lars Liden, Jianfeng Gao, Matthew P. Lungren, Tristan Naumann, Sheng Wang, and Hoifung Poon. Biomedclip: a multimodal biomedical foundation model pretrained from fifteen million scientific image-text pairs, 2024. URL https://arxiv.org/abs/2303.00915.

Lianmin Zheng, Wei-Lin Chiang, Ying Sheng, Siyuan Zhuang, Zhanghao Wu, Yonghao Zhuang, Zi Lin, Zhuohan Li, Dacheng Li, Eric. P Xing, Hao Zhang, Joseph E. Gonzalez, and Ion Stoica. Judging llm-as-a-judge with mt-bench and chatbot arena, 2023.